Numerical Investigation of Multijet Air Impingement on Pin Fin Heat Sink with Effusion Slots

N. K. Chougule G. V. Parishwad A. R. Nadgire

Abstract— **The work reported in this paper is an attempt to enhance heat transfer in electronic devices with use of multi air jet impingement on pin fin heat sinks with effusion slots on the nozzle plate. In this study the effect of nozzle jet exit velocity, heat sink array, and the height of pin fin on the average Nusselts number (Nu_a) are studied. Numerical investigation is carried out on multi air jet array of 3x3, 5x5 and 10x10(nozzle diameter 5, 3 and1.5mm) impinging on aluminum pin fin heat sink (pin fin array 4x4, 6x6 and 11x11 respectively) for *H/d* ratio of 3, 4 and 5 keeping the nozzle exit to pin fin tip distance 1d for each case. Numerical analysis carried out for the Reynolds number range from 11000 to 49000 for constant heat supply of 30W (Constant heat flux 8333W/m^2). The results reveals that the at smaller *H/d* ratio heat transfer is more effective. Similarly the smaller the pin fin size, better the heat transfer performance of pin fin heat sink. The higher Reynolds number yields more heat transfer coefficient.**

Index Terms— electronic cooling, multijet impingement, Pin fin heat sink, effusion slots.

I. Introduction

JET impingement systems provide an effective means for the enhancement of convective processes due to the high heat and mass transfer rates that can be achieved. Extensive research has been conducted on jet impingement to understand their heat and mass transfer characteristics. However, there are few studies on the effect of fin height on heat transfer in multijet impingement and on spent air through effusion slot have been carried out. Due to this gap and probably effective solution to heat transfer enhancement problem, jet impingement heat transfer with effusion slots is being investigated in this study. Thus the present study involves a numerical investigation of heat transfer characteristic of finned heat sink using multi air jet impingement with effusion slots, expecting the higher heat transfer coefficient. A numerical study is carried out using commercial CFD code ANSYS ICEM CFX as the platform.

For the conventional array impinging jets, a crossflow is formed by the spent air from the impinging jets in a confined space, and the amount of the cross-flow increases as the flow moves downstream. Turbulence intensity of impinging jets is increased because the crossflow disturbs impinging jets at downstream region. Therefore, the local heat/mass transfer rate around the stagnation region is enhanced. However, at the mid-way region, the heat/mass transfer coefficients are decreased because the thermal boundary layer develops in the cross-flow at this region and flow pattern is similar to the duct flow [1]. Therefore, the heat/mass transfer coefficients are non-uniform over the overall impingement surface.

A. Literature review

Cho and Goldstein [2] and Cho and Rhee [3] investigated the effect of hole arrangements on local heat/mass transfer characteristics for the array jet impingement with spent air removal through the effusion holes on the target plate. They found that the high transfer rate is induced by strong secondary vortices and flow acceleration, and the overall transfer rate is approximately 45–55% higher than that for impingement cooling alone.

Hollworth and Dagan [4], [5] measured the average and local heat transfer coefficients of arrays of turbulent air jets impinging on perforated target surfaces, and reported that arrays with staggered vents consistently yield 20–30% higher heat transfer rates than do the impinging jets on the solid plates.

Huber and Viskanta [6] studied the effect of spent air exit in the orifice plate on the local and average heat transfer for 3x3 square array jet with 2x2 square spent air exit using the liquid crystal technique. They found that the interaction of adjacent impinged jets is reduced by spent air and the heat transfer on target plate is more enhanced. They also investigated the effect of jet-to-jet spacing on the heat transfer; it was found that, for large plate spacing, jet interference causes a significant degradation of the heat transfer [1].

Huang [7] studied the effect of spent air flow direction on impingement heat transfer, when the feeding flow is parallel to the spent flow. They found when the spent flow has an opposite direction to incoming flow, Nusselts number peak occurs at leading section of the heat transfer target wall. When spent flow has the same direction as the incoming flow, the Nusselts number at the trailing part will slightly higher than the leading part, but with overall performance 40% lower.

Dong-Ho Rhee [8] investigated the effects of spent air flows with and without effusion holes on heat/mass transfer on a target plate for array impinging jets and reported that for small gap distances, heat/mass transfer coefficients without effusion holes are very non-uniform due to the

N. K. Chougule, Department of Mechanical Engineering, College of Engineering Pune, India. (chougulenk@gmail.com)
G. V. Parishwad Department of Mechanical Engineering, College of Engineering Pune, India. (gvp.mech@coep.ac.in)
A. R. Nadgire, Department of Mechanical Engineering, MIT College of Engineering, Pune, India. (anand.nadgire@gmail.com)

ISBN: 978-988-19253-1-2
ISSN: 2078-0958 (Print); ISSN: 2078-0966 (Online)

strong effects of cross-flow and Re-entrainments of spent air. However, uniform distributions and enhancements of heat/mass transfer coefficients are obtained by installing the effusion holes. However, there is no work has been carried out to investigate the performance of heat sinks with multijet impinging on a heat sink and then discharging air through effusion slots provided on the nozzle plate, especially with the numerical technique.

II. Problem Description

The schematic of a multi jet impinging on a pin fin heat sink which is to be analyzed is shown in Fig.1. The air jet is discharged through the round nozzle having length *l* and diameter *d* is directed normally towards the pin finned target plate with base *60 x 60 x 6mm*, the pin fin are provided on top of plate on *50 x 50mm* area, the sink is subjected to constant heat input *(30W)* from bottom and except top surface all other walls are adiabatic. The material of the heat sink is *Aluminum*. The jet after impingement spent air will exit from opening provided in top confinement plate in opposite to impinging direction as shown in Fig. 1.

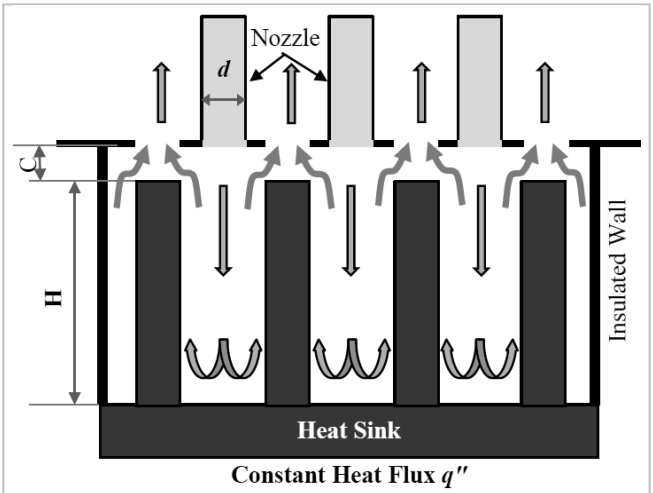

Fig. 1 Schematic of multi jet impingement on pin fin heat sink

The air flow rate, pin fin height, the diameter of the jet and pin fin, and jet to target surface distance are the main variables, which can be chosen to solve a given heat and mass transfer problem. Reynolds number is varied in turbulent range to study the effect of *Re* on heat transfer coefficient. Jet exit area for each geometry of nozzle plate is maintained same for different jet diameters and pin fin arrangement. Three different jet arrays - *3x3, 5x5, 10x10* are considered keeping jet exit flow area constant – *1d*, and three different fin height to diameter ratios *H/d – 3, 4, 5* are considered. Reynolds number is varied in large range *11000 to 49000* to study its effect on heat transfer coefficient. Reynolds number based on diameter gives different volume flow rate for same Reynolds number for different jet diameters. Thus to generalize the Reynolds number for different jet diameters with same exit flow rate, Reynolds number is calculated by using square root of jet area as characteristics diameter.[9]

III. EXPERIMENTAL DETAILS

A schematic diagram of the experimental set up is shown in Fig.1. It is an Air flow bench, which provides controlled and measurable flow of air through nozzles or jet plate directed towards the target plate. It consists of a 0.5 HP blower, air straightener (air box), contraction section, and structure and Data Acquisition System (DAQ) to measure temperature, pressure.

The blower draws air from the atmosphere and delivers it along a pipe to an air box, which is above the test area. There is honeycomb structure inside the air box in order to provide streamlined flow prior to impinging on the heat sink and a butterfly valve used in order to regulate the discharge from the centrifugal blower.

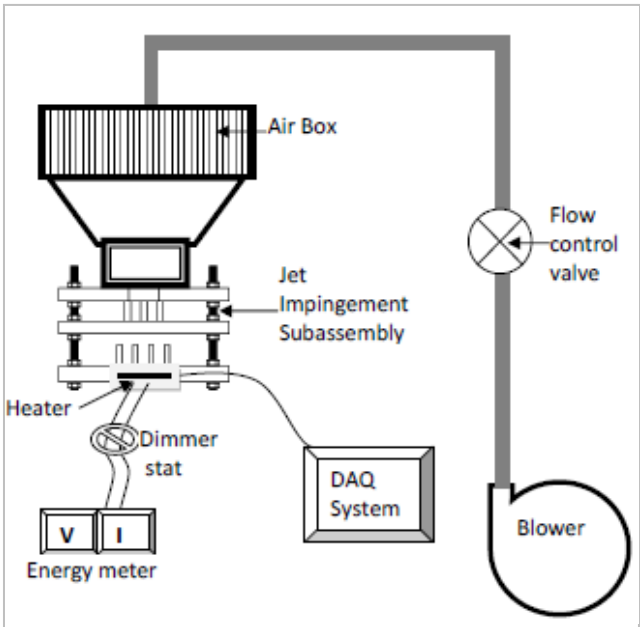

Fig. 2 Experimental set up

Contraction section attached to air box, directs the streamlined air flow to jet impingement assembly. This jet impingement assembly consists of nozzle plate, heater section, heat sink and mechanism to control the distance between the nozzle plate and the heat sink (Z/d ratio). There is provision in jet assembly to obtain minimum crossflow, semi crossflow, strong crossflow and maximum crossflow.

The air flow bench structure is made to incorporate other devices such as DAQ system, Power supply, pressure measurement devices and various controls. Micro-manometer is used to measure the static pressure of air at the outlet of the jet at different locations. K-type thermocouples are used to measure the temperature. Average of all the readings is taken and jet velocity is calculated. To measure the temperature at the base of the fin, 8K type thermocouples (30 gauges) are mounted on base through 1 mm diameter hole and 2 on the tip of pin.

IV. Numerical Modeling

A. Turbulence modeling - The SST turbulence model

The SST model combines the advantages of the *k-ε* and the *k-ω* model to achieve an optimal model formulation for a wide range of applications. For this a blending function F1 is introduced which is equal to one near the solid surface and equal to zero for the flow domain away from the wall. It activates the *k-ω* model in the near wall region and the *k-ε* model for the rest of the flow. By this approach the attractive near-wall performance of the *k-ω* model can be used without

ISBN: 978-988-19253-1-2
ISSN: 2078-0958 (Print); ISSN: 2078-0966 (Online)

the potential errors resulting from the free stream sensitivity of that model. In addition, the SST model also features a modification of the definition of the eddy viscosity, which can be interpreted as a variable c_μ, where c_μ in the *k-ε* model is constant. This modification is required to accurately capture the onset of separation under pressure gradients. In addition to the advanced turbulence models, an advanced near wall treatment has been developed and implemented into CFX, which allows the user to benefit from the advantages of the model.

In study of J. Badra, [10] the SST *k-ω* model showed that it can describe this kind of problems the in the best way. In this study SST (Shear-Stress Transport) turbulence model has used because some authors had already found in the previous study that SST turbulence model implemented in CFX provided better agreements with the internal heat transfer coefficients measured inside a cooling device similar to that of the present study.

B. Geometry and Meshing

The geometry and meshing is created in *ANSYS ICEM CFD* as it maintains close relationship with geometry during mesh generation and post processing. *ANSYS ICEM CFD* provides direct link between geometry and analysis. As geometry is small enough so here we consider complete geometry for the CFD analysis (Fig. 3). All geometrical dimensions are similar as that of test set up.

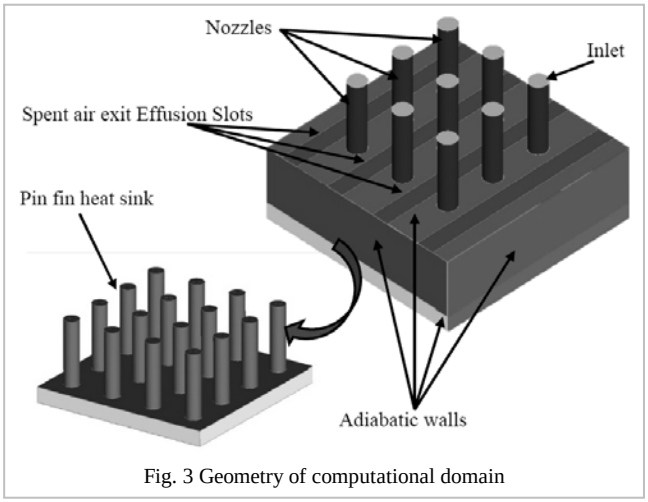

Fig. 3 Geometry of computational domain

The multiblock structured hexahedral mesh is used as orthogonally is maintained hence accurate prediction of heat transfer characteristics there. To capture the near wall flow phenomenon, dense hexahedral mesh at near wall region is created by using the linear mesh law algorithm. This was not only capture the near wall flow phenomenon but also increases the smoothness of the mesh. Dense mesh also helps to control the y^+ character. The Quality, Determinant, Aspect Ratio etc. are maintained above the standard valued mentioned by ANSYS ICEM user guide. [26]. Grid independency on heat transfer characteristics was checked by changing the element size from 0.2 million to 0.4 million which follows that about 0.3 million was good enough for resent analysis from view point of accuracy and computational time.

At nozzle inlet the *Pressure Inlet (subsonic)* boundary condition is used; for all sides the *Adiabatic Wall* boundary condition is used; at base of pin fin heat sink *Constant Heat Flux* (30W) is applied; at interface of air and heat sink the *Conservative Interface Flux* condition is applied.

C. Numerical procedure

In this work the flow field is numerically examined by using *ANSYS CFX*. Geometry creation and meshing is performed in *ANSYS ICEM CFD*. A mesh file is imported in the *CFX-Pre*, where boundary conditions applied and setting of the turbulence module and other setting for *CFX-Pre* is done. The flow and turbulent fields have to be accurately solved to obtain reasonable heat transfer predictions. Higher resolution scheme is used for all terms that affect heat transfer. Higher order discretization scheme is used for the pressure; momentum, turbulent kinetic energy, specific dissipation rate, and the energy. Flow, turbulence, and energy equations have been solved.

The mesh is having two domains *fluid (air)* and *solid (Al)* domain. In the fluid domain the *inlet* boundary condition is specified the measured velocity and static temperature (300K) of the flow were specified at the inlet of the nozzle. *No-slip condition* was applied to the wall surface. In fluid domain there is also *opening* boundary condition in which flow regime is subsonic, relative pressure is 0 Pa with operating temperature (300 K) and the turbulence intensity of 5%. In solid domain the *constant heat flux* (8333W/m^2) was given with the initial temperature condition 40°C at the base of heat sink and the sides of heat sink base plat are adiabatic. At the fluid solid domain interface *conservative heat flux* boundary condition is applied. The variation of thermal and physical properties of air with temperature is neglected. The flow field was numerically examined by use of CFX (ANSYS), assuming the steady-state flow.

V. Results And Discussions

A. Validation with Experimental Results

A comparison between experimental and CFD results are shown in Table 1. To validate CFD results, the detailed experimentation were carried out on 4x4 pin fin heat sink array (d_p=5mm) with *H/d* ratios 3d, 4d, 5d with Reynolds number 19000, 25000 and 31000. The average temperature obtained from the experimental data is used to validate the computational work. To simulate the above experimental conditions in context of CFD analysis, the same geometry, boundary conditions are applied and also temperature monitoring points are located at the same position where thermocouples are physically located. Mostly within all the range of parameters, it is observed that CFD results are in good agreement with experimental results.

TABLE 1
Percentage Agreement between Experimental and CFD results

H/d ratio	*Re*	Experimental	Numerical	Percentage Agreement
		Nu_{avg}	Nu_{avg}	Nu_{avg}
5	18896	82.86	93.53	87.07
5	25116	93.40	104.10	88.49
5	31049	100.93	115.52	85.48
4	18896	90.49	100.90	88.44
4	25116	100.29	112.48	87.79
4	31049	109.02	124.94	85.34
3	18896	98.29	109.51	88.53
3	25116	107.92	121.71	87.17
3	31049	120.09	134.71	87.77

ISBN: 978-988-19253-1-2
ISSN: 2078-0958 (Print); ISSN: 2078-0966 (Online)

B. Comparison with conventional method

The results obtained from effusion slot arrangement are compared with conventional minimum crossflow arrangement (Table 2). The multijet air impingement for *4x4* heat sink with *Z/d=6* with effusion slots is compared with minimum crossflow scheme for. It is found that the effusion slot arrangement gives 20 to 52% enhancement over conventional method. It is observed that heat transfer performance of multi jet impingement with effusion slot is more efficient at lower Reynolds number.

TABLE 2
COMPARISON OF MINIMUM CROSSFLOW AND EFFUSION SLOT SCHEME

	Nu_{avg}		
Re	**Minimum crossflow**	**Effusion slot**	**% Enhancement**
5	18896	82.86	93.53
5	25116	93.40	104.10
5	31049	100.93	115.52
4	18896	90.49	100.90
4	25116	100.29	112.48
4	31049	109.02	124.94
3	18896	98.29	109.51
3	25116	107.92	121.71
3	31049	120.09	134.71

C. Effect of Re on average Nusselts number

Figure 4 shows average Nusselts number variation with respect to Reynolds number. It is observed that the Nusselts number is directly proportional to Reynolds number. At higher Reynolds number, its effect on Nusselts number is more pronounced.

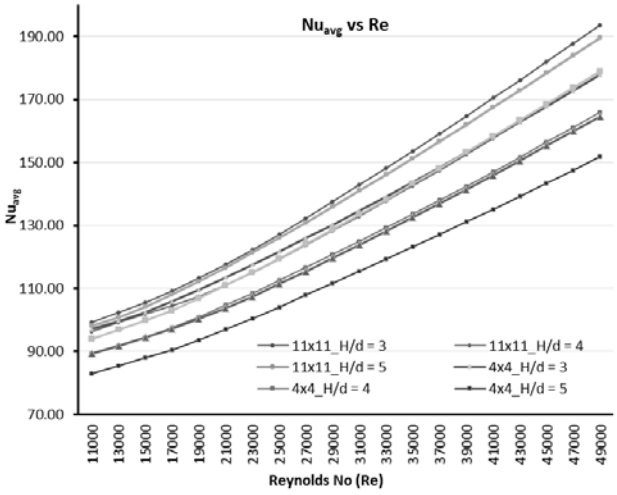

Fig. 4 Effect of Re and H/d on average Nusselts number (Nu_{avg})

D. Effect of H/d on average Nusselts number

Figure 5 shows the effect of *H/d* ratio on average Nusselts number at different Reynolds number. With decreasing *H/d* ratios the Nusselts number increases accordingly. The *H/d*=3 shows 5 – 20% enhancement over *H/d*=5 for same Reynolds number. It is observed from vector plot that there is more vortex flow in the wall jet region near the target surface at lower Reynolds number, this increases heat transfer coefficient. Also at smaller *H/d* ratios the jet strikes directly on target surface without losing its much momentum with surrounding flow, this results in the jet reaching the target surface with higher momentum, this increases the heat transfer coefficient.

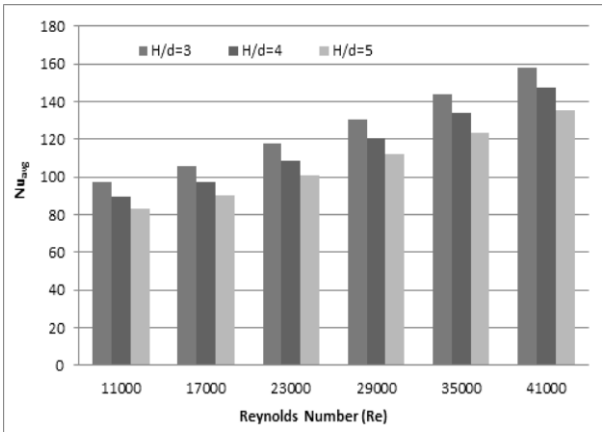

Fig. 5 Effect of H/d ratio on average Nusselts number (Nu_{avg})

E. Velocity variation

The Figure 6 shows the vector plots at *Re = 49000* for 3x3 pin fin heat sink. After closely observing the velocity contours, it is found that the at smaller *H/d* ratios, boundary layer thickness is small in the wall jet region; the smaller boundary layer higher the heat transfer coefficient. It is observed that at smaller *H/d* ratios, there is vortex flow near to wall jet region; that also leads to increase in heat transfer coefficient.

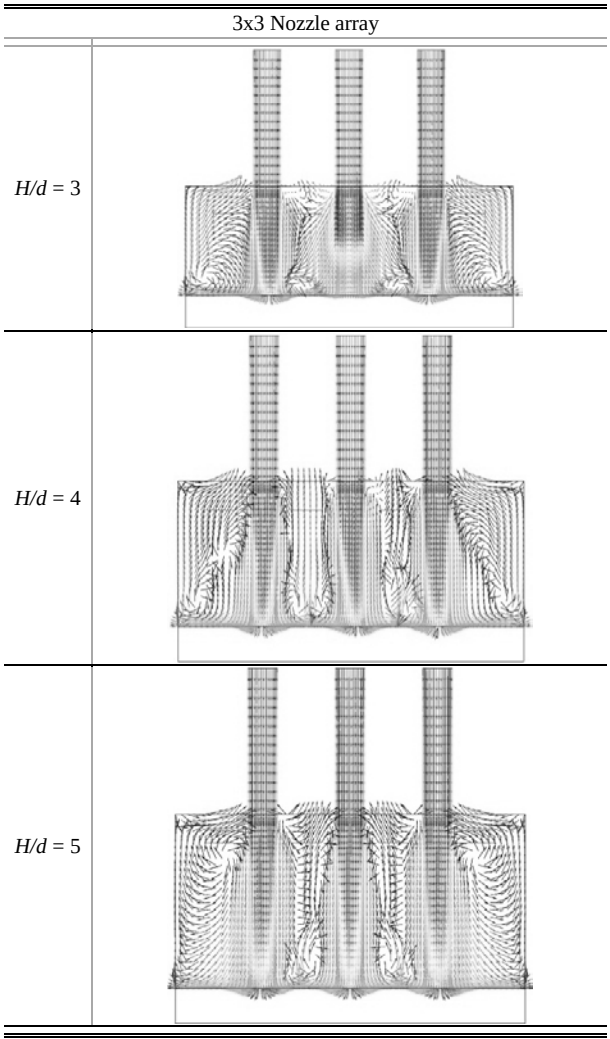

Fig. 6 Effect of Re and H/d on average Nusselts number (Nu_{avg})

ISBN: 978-988-19253-1-2
ISSN: 2078-0958 (Print); ISSN: 2078-0966 (Online)

F. Effect of H/d ratio on Temperature Distribution

The temperature contours of all the geometries for Re = 49000 are shown below (Fig. 7) as higher heat transfer coefficient is observed at this Reynolds number. Typical temperature distribution on the centerline passing through stagnation point as a function of radial distance for different *H/d* ratio. From temperature distribution it is clear that at smaller *H/d* ratios (*H/d*=3) the temperature on target surface is lowered and more uniform. It is also observed that for smaller pin fin diameter the temperature distribution is uniform and average temperature of target surface is also lowered with decreasing *H/d* ratio. On base plate pin fins are distributed on 50x50mm area, thus temperature outside this area is higher than fined area. The temperature variation in finned area is in range of 301 to 305K.

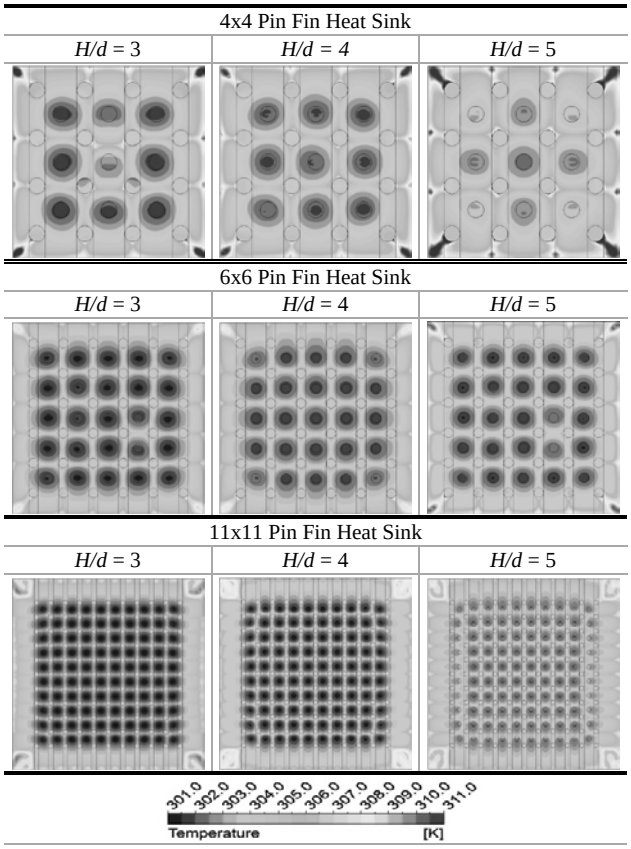

Fig. 7 Temperature contours *(Re = 49000)*

VI. Conclusion

After studying the results obtained numerical and experimental method following points are concluded:

- *H/d* ratio had a significant impact on heat transfer. At smaller *H/d* ratios with higher *Re*, there is vortex flow near the target surface in wall jet region, causing increase in heat transfer coefficient. At *H/d=3*, average base temperature is much lower, compared to other cases.
- For a given *H/d* ratio, the same temperature contours are observed only temperature range is varying. At smaller *H/d* ratio more uniform target surface temperate is obtained.
- More turbulences is observed at higher *Re* which helps to enhance heat transfer. At higher *Re* the Nu_{avg} increases but on other side flow become wavy and diverts from the target impingement.
- Pin fin diameter has significant impact on Nusselts number, smaller the diameter of pin fin better the heat transfer coefficient.
- Ultimately, CFD results are validated by experimentations to determine overall error in predicting real situation, CFD results shows good agreement with experimental results (85 – 89% agreement).

• Nomenclatures

d	Nozzle diameter, m
h_{avg}	heat transfer coefficient, W/m^2K
Nu_{avg}	Average Nusselt number, hL/k.
Re	Reynolds number based on jet exit diameter $= \rho Vd/\mu$
V	Mean velocity at jet exit, m/s
Z	Distance between nozzle exit and impinging plate, m
H/d	Dimensionless jet to target plate spacing

References

[1] Huber, A.M. and Viskanta, R. (1994). *"Effect of jet–jet spacing on convective heat transfer to confined, impinging arrays of axisymmetric jets"*, Int. J. Heat Mass Transfer 37, 2859–2869.

[2] H. H. Cho, R. J. Goldstein, *"Effect of hole arrangements on impingement/effusion cooling"*, Proceeding of 3rd KSME-JSME Thermal Engineering Conference, pp. 71–76, 1996.

[3] H. H. Cho, D. H. Rhee, *"Local heat/mass transfer measurement on the effusion plate in impingement/effusion cooling system"*, Trans. ASME, J. Turbomach, 601–608, 2001.

[4] B. R. Hollwarth, L. Dagan, *"Arrays of impinging jets with spent fluid removal through vent holes on the target surface. Part 1: average heat transfer"*, Trans. ASME, J. Eng. Power 102 (1980) 994–999.

[5] B. R. Hollwarth, G. Lehmann, J. Rosiczkowski, *"Arrays of impinging jets with spent fluid removal through vent holes on the target surface. Part 2: local heat transfer,"* Trans. ASME, J. Eng. Power 105 (1983) 393–402.

[6] Huber A. M., Viskanta R. *"Convective Heat Transfer to a Confined Impinging Arrays of Air Jets with Spent Air Exits"* J. Heat Transfer, Vol. 116, pp. 570-576, 1994.

[7] Huang G. C. "Investigations of Heat Transfer Coefficient for Air Flow Through Round Jets Impinging Normal to a Heat Transfer Surface" J. Heat Transfer, Vol. 85, pp. 237-245, 1963.

[8] Dong-Ho Rhee, Pil-Hyun Yoon, Hyung Hee Cho, *"Local heat/mass transfer and flow characteristics of array impinging jets with effusion holes ejecting spent air"*, International Journal of Heat and Mass Transfer 46, 1049-1061, 2003.

[9] Young K., Myung H., and Kwan-Soo Lee, *"Heat Removal by Aluminum-Foam Heat Sinks in a Multi-Air Jet Impingement"*, IEEE transaction on advanced packing, 2005.G. Theoclitus, *"Heat-transfer and flow-friction characteristics on nine pin-fin surfaces"*, J. Heat Transfer, 383–390, 1966.

[10] Badra J, A. R. Masri, M. Freeman, and M. Fitch *"Enhanced Heat Transfer from Arrays of Jets Impinging on Plates"* 16th Australasian Fluid Mechanics Conference Crown Plaza, Gold Coast, Australia, 2007.

ISBN: 978-988-19253-1-2
ISSN: 2078-0958 (Print); ISSN: 2078-0966 (Online)